

# Dynamic Characteristics of Active Magnetic Bearing System on Turbine Expander

Zhenyu Xie Longxiang Xu

College of Mechanical Engineering, Nanjing University of Aeronautics and Astronautics,  
Nanjing, China, 210016, xiezy@nuaa.edu.cn

Damou Qiu Lie Yu

College of Mechanical Engineering, Xi'an Jiaotong University,  
Xi'an, China, 710049

## ABSTRACT

An active magnetic bearing (AMB) system has been successfully developed for turbine expander by our laboratory. Dynamic characteristics of the system are studied by theoretical analysis and experiment investigation in this paper. The relationships among stiffness, damping, stability, innate frequency and control parameters are discussed. The results show that the scope of the stiffness and damping of the AMBs is limited by the system stability. Both the cylindrical and conical innate frequencies are sensitive to the control parameters, while the first innate bending frequency is less sensitive. On the other hand, the adjustment of the control parameters and the increase of the damping of the AMBs can restrain vibration of the rotor rotating at the cylindrical and conical innate frequencies, while the damping of the AMBs is too little to keep the rotor rotating normally when the rotor operates near the first bending innate frequency.

## INTRODUCTION

Compared with traditional bearings, AMB has many advantages, such as noncontact supporting and active control capabilities. The number of AMB equipped rotating machines has been increasing remarkably in the last few years [1].

AMB is mainly applied on rigid rotor system, and now gradually applied on flexible rotor system [2]. However, there are many difficulties for AMB

to be applied on practical flexible rotor system. The magnetic bearing system may have extremely light damping [3], which can not restrain the vibration of the rotor when it passes the bending critical speeds. So-called non-co-location problem of sensor and electromagnet in radial AMB usually occurs due to limited space around the rotor and it could cause the entire rotor system instability especially combined with 1<sup>st</sup> and 2<sup>nd</sup> bending mode [4].

Modern control theories, i.e., the LQR theory,  $H^\infty$  theory, sliding-mode theory and so on, are prepared for the optimal control design for the servo feedback system. However, it seems that they are too general for practical use of the high-speed flexible rotor, and the passage of the bending mode resonance is generally difficult [2]. Special approaches have to be adopted for practical system to pass the bending critical speed, such as Feed Forward excitation method [2, 5-8], Ncross method [2], disturbance observer [9], HB type magnetic bearing [10], sensor averaging and actuator averaging [4]. To avoid encountering this kind of problem, some application instances adopt rigid-rotor-design method [2, 11].

This paper presents our practical AMB system developed for turbine expander, whose flux of atmosphere is 3200m<sup>3</sup>/h, and the rotor reaches 30000r/min. In this application, the rotor is about 13 kilogram, and is fully supported by the AMBs in all five degrees of freedom. Ten eddy-current sensors are used to detect the displacements of the rotor in

five degrees of freedom in a differential structure, and another one sensor is used to detect the rotation speed of the rotor. TMS320F240 is engaged here as the hardware of the controller, and the classic PID control layout is used. Five switch power amplifiers are used to drive the currents through the wires, and the power supply of each switching amplifier is 150 volt. The maximum current in each coil is 5 ampere.

Also, the rigid-rotor-design method is adopted in the design of turbine expander in order to avoid encountering the problem of flexible rotor. This paper discusses the dynamic characteristics of the practical AMB system, when the rotor rotates near the 1<sup>st</sup> bending critical speed. Analysis and experiment results are presented in detail.

### SYMBOLS AND NOTATIONS

- $k_{ri}$ : current stiffness coefficient
- $A_s$ : plus coefficient of sensor segment
- $T_s$ : time constant of displacement segment
- $A_p$ : plus coefficient of amplifier segment
- $T_p$ : time constant of power amplifier segment
- $k_p$ : proportional coefficient of controller
- $k_i$ : integral coefficient of controller
- $k_d$ : differential coefficient of controller
- $T_d$ : differential time coefficient of controller
- $i_x, i_y$ : control current in AMBs of  $x, y$  freedom

### MODEL OF MATHEMATICS

In the AMB rotor system,  $x, y, z, \mathbf{j}, \mathbf{y}$  are displacements in five degrees of freedom, respectively. For convenience, we introduce non-dimensional parameters as follows,

$$\bar{x} = x/d_0, \quad \bar{y} = y/d_0, \quad \bar{\mathbf{j}} = \mathbf{j},$$

$$\bar{\mathbf{y}} = \mathbf{y}, \quad \bar{i}_x = i_x/i_0, \quad \bar{i}_y = i_y/i_0$$

where,  $i_0$  is average control current,  $d_0$  average diameter. The rotor is divided into a set of nodes, and the total number of nodes is 31. The magnetic bearings are on the 11<sup>th</sup> and 22<sup>nd</sup> node, respectively. Non-dimensional equation of the system can be written as follows,

$$\begin{bmatrix} 0 & \bar{M} & 0 \\ \bar{M} & \bar{C} & 0 \\ \bar{K}_{z1} & \bar{K}_{z2} & \bar{K}_{z3} \end{bmatrix} \dot{R} + \begin{bmatrix} -\bar{M} & 0 & 0 \\ 0 & \bar{K} & \bar{K}_{zi} \\ 0 & \bar{K}_{z4} & \bar{K}_{z5} \end{bmatrix} R = 0 \quad (1)$$

where,  $R = [R_1, R_2, R_3]^T$ ,  $\bar{M}, \bar{C}$  and  $\bar{K}$  are non-dimensional matrixes of mass, damping, and stiffness, respectively.  $\bar{K}_{zi}$  is related to  $k_{ri}$ .  $\bar{K}_{z1}, \bar{K}_{z2}, \bar{K}_{z3}, \bar{K}_{z4}$  and  $\bar{K}_{z5}$  are functions of  $A_s, T_s, A_p, T_p, k_p, k_i, k_d$  and  $T_d$ .

Here,

$$R_1 = [\dot{\bar{x}}_1, \dot{\bar{y}}_1, \dot{\bar{\mathbf{j}}}_1, \dot{\bar{\mathbf{y}}}_1, \dot{\bar{x}}_2, \dot{\bar{y}}_2, \dot{\bar{\mathbf{j}}}_2, \dot{\bar{\mathbf{y}}}_2, \dots, \dot{\bar{x}}_{31}, \dot{\bar{y}}_{31}, \dot{\bar{\mathbf{j}}}_{31}, \dot{\bar{\mathbf{y}}}_{31}]^T$$

$$R_2 = [\bar{x}_1, \bar{y}_1, \bar{\mathbf{j}}_1, \bar{\mathbf{y}}_1, \bar{x}_2, \bar{y}_2, \bar{\mathbf{j}}_2, \bar{\mathbf{y}}_2, \dots, \bar{x}_{31}, \bar{y}_{31}, \bar{\mathbf{j}}_{31}, \bar{\mathbf{y}}_{31}]^T$$

$$R_3 = [\bar{i}_{x11}, \bar{i}_{y11}, \bar{i}_{x11}, \bar{i}_{y11}, \bar{i}_{x22}, \bar{i}_{y22}, \bar{i}_{x22}, \bar{i}_{y22}]^T$$

### CALCULATION RESULTS

Control parameters of the system are shown as Table 1.

TABLE 1: Control parameters of the System

	$k_p$	$k_i$	$k_d$	$T_d$ (s)
Thrust Bearing	1.4	10.6	$2.2 \times 10^{-3}$	$4.6 \times 10^{-5}$
Radial Bearings	3.8	35.5	$1.4 \times 10^{-3}$	$2.0 \times 10^{-5}$

Within 0~100000rpm, the calculation results of the innate critical speeds are shown as follows,

$$N_1 = 4310 \text{ rpm}, \quad N_2 = 6100 \text{ rpm}, \\ N_3 = 37740 \text{ rpm}, \quad N_4 = 74940 \text{ rpm}$$

The corresponding rates of logarithmic attenuation are as follows,

$$\mathbf{d}_1 = 0.988, \quad \mathbf{d}_2 = 1.02,$$

$$\mathbf{d}_3 = 5.87 \times 10^{-3}, \quad \mathbf{d}_4 = 0.111$$

Varying  $k_p$  and  $k_d$ , the relationships of critical speeds to the  $k_p$  and  $k_d$  can be obtained as Fig.1.

### EXCITING VIBRATION TEST

In the Test 1, Test 2 and Test 3, the rotor is

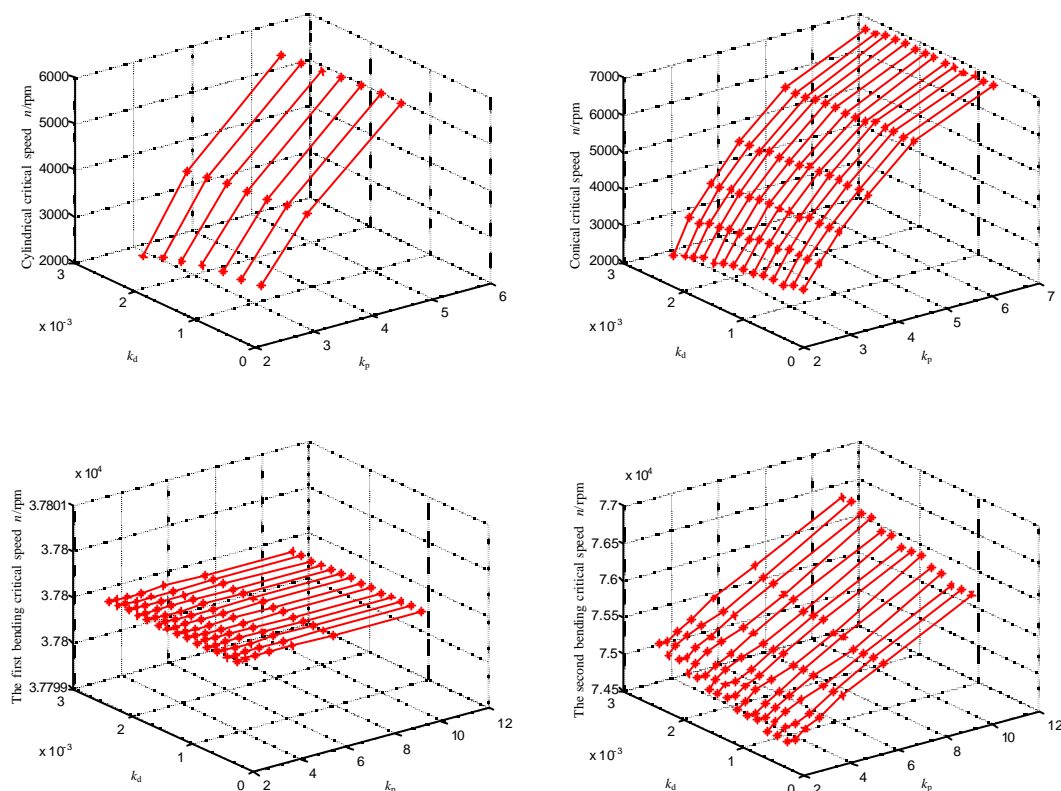


FIGURE 1: Sensitivity of critical speeds to  $k_p$  and  $k_d$

supported by AMBs normally, and the control parameters with various differential parameters are shown in Table 2. Adding sinusoidal signal with various frequencies to the input of the power amplifier, exciting force with various frequencies can be brought into the system. Based on the amplitude of the rotor, curves of flexibility corresponding to the differential parameters can be obtained as shown in Fig.2.

TABLE 2: Control parameters in Test 1, 2 and 3

	$k_p$	$k_i$	$k_d$	$T_d$ (s)	
Thrust Bearing	1.4	10.6	$2.2 \times 10^{-3}$	$4.6 \times 10^{-5}$	
Radial Bearings	Test 1	2.4	35.5	$4.9 \times 10^{-4}$	$1.4 \times 10^{-5}$
	Test 2	2.4	35.5	$8.8 \times 10^{-4}$	$1.7 \times 10^{-5}$
	Test 3	2.4	35.5	$1.6 \times 10^{-3}$	$2.2 \times 10^{-5}$

In the Test 4, Test 5 and Test 6, the rotor is supported by AMBs normally, and the control parameters with various proportional parameters are

shown in Table 3. Also, curves of flexibility corresponding to the various proportional parameters can be obtained as shown in Fig.3.

TABLE 3: Control parameters in Test 4, 5 and 6

	$k_p$	$k_i$	$k_d$	$T_d$ (s)	
Thrust Bearing	1.4	10.6	$2.2 \times 10^{-3}$	$4.6 \times 10^{-5}$	
Radial Bearings	Test 4	2.4	35.5	$1.6 \times 10^{-3}$	$2.2 \times 10^{-5}$
	Test 5	2.9	35.5	$1.6 \times 10^{-3}$	$2.2 \times 10^{-5}$
	Test 6	3.6	35.5	$1.6 \times 10^{-3}$	$2.2 \times 10^{-5}$

From Fig.2 and Fig.3, we can conclude that,

- (1) There are two innate frequencies near 100Hz and 640Hz. The innate frequencies over 1000Hz are larger enough than the operation speed and can be ignored.
- (2) The value of innate frequencies near 640Hz can not be varied by the adjustment of the control parameters.

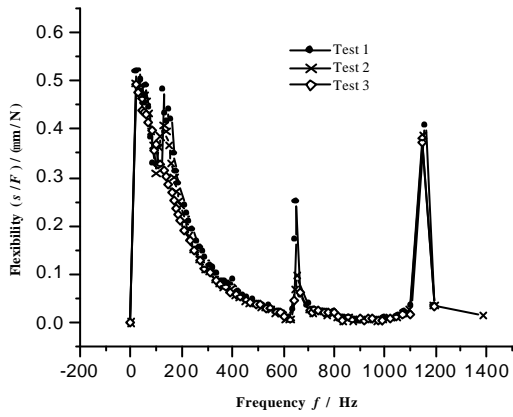


FIGURE 2: Curves of flexibility in Test 1, 2 and 3

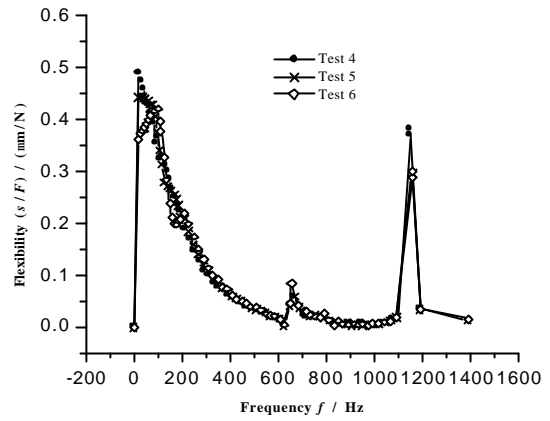
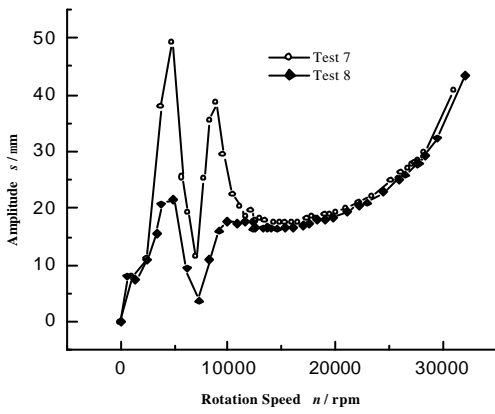
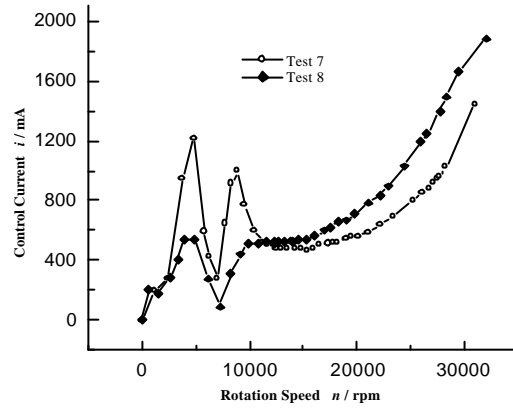


FIGURE 3: Curves of flexibility in Test 4, 5 and 6

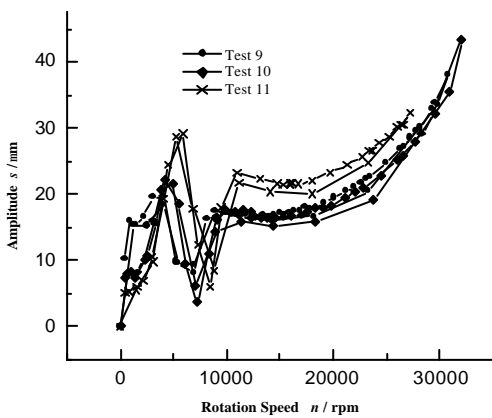


(a)

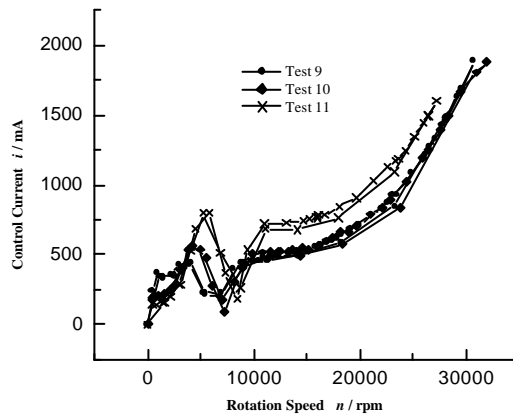


(b)

FIGURE 4: Curves of vibration (a) and control current (b) in Test 7 and Test 8



(a)



(b)

FIGURES5: Curves of vibration (a) and control current (b) in Test 9, Test 10 and Test 11

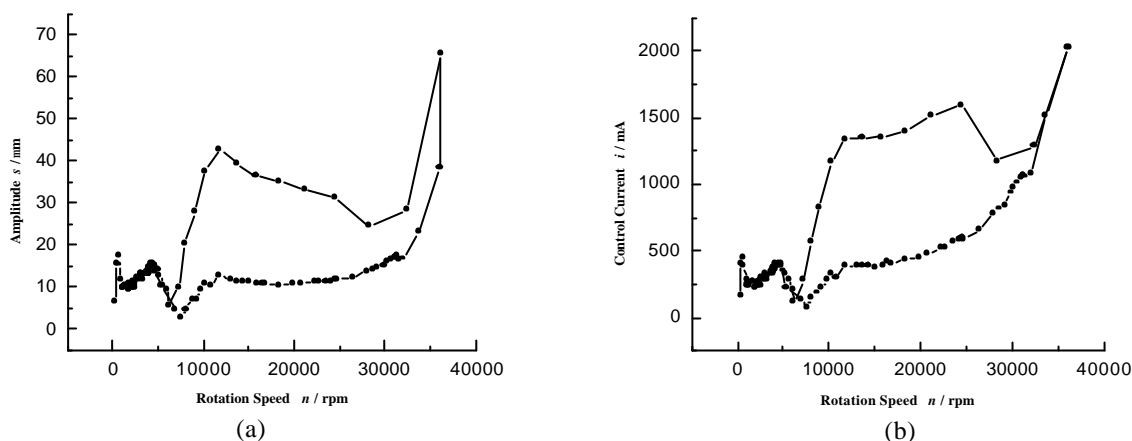


FIGURE 6: Curves of vibration (a) and control current (b) in Test 12

**OPERATION TEST**

In the Test 7 and Test 8, the turbine expander supported by the AMBs operates with high rotation speed, and the control parameters with various differential parameters are shown in Table 4. Fig.4 shows the amplitude of the rotor corresponding to the various differential parameters measured by 1# sensor, and the amplitude of control current in 1# radial bearing.

TABLE 4: Control parameters in Test 7 and 8

		$k_p$	$k_i$	$k_d$	$T_d$ (s)
Radial Bearings	Thrust Bearing	1.4	10.6	$2.2 \times 10^{-3}$	$4.6 \times 10^{-5}$
	Test 7	2.7	35.5	$5.5 \times 10^{-4}$	$1.5 \times 10^{-5}$
	Test 8	2.7	35.5	$1.1 \times 10^{-3}$	$1.8 \times 10^{-5}$

TABLE 5: Control parameters in Test 9, 10 and 11

		$k_p$	$k_i$	$k_d$	$T_d$ (s)
Radial Bearings	Thrust Bearing	1.4	10.6	$2.2 \times 10^{-3}$	$4.6 \times 10^{-5}$
	Test 9	2.4	35.5	$1.1 \times 10^{-3}$	$1.8 \times 10^{-5}$
	Test 10	2.7	35.5	$1.1 \times 10^{-3}$	$1.8 \times 10^{-5}$
	Test 11	3.0	35.5	$1.1 \times 10^{-3}$	$1.8 \times 10^{-5}$

In the Test 9, Test 10 and Test 11, the turbine expander operates with high rotation speed, and the

control parameters with various proportional parameters are shown in Table 5. Fig.5 shows the amplitude of the rotor corresponding to the various proportional parameters measured by 1# sensor, and the amplitude of control current in 1# radial bearing.

Fig.4 and Fig.5 show that the system has two critical speeds below 10000rpm and another critical speed above 30000rpm. The value of the critical speed above 30000rpm is less influenced by the adjustment of the control parameters.

To further validate above, the system operates near the first bending critical speed in Test 12, and the control parameters are shown in Table 6. Both the amplitude of the rotor measured by 1# sensor, and the amplitude of control current in 1# radial bearing are shown in Fig.6.

TABLE 6: Control parameters in Test 12

	$k_p$	$k_i$	$k_d$	$T_d$ (s)
Thrust Bearing	1.4	10.6	$2.2 \times 10^{-3}$	$4.6 \times 10^{-5}$
Radial Bearings	3.8	35.5	$1.4 \times 10^{-3}$	$2.0 \times 10^{-5}$

Fig.6 shows that, when the rotation speed reach 36188rpm, the amplitude of the rotor and control current are too large to keep the rotor operating normally, and the rotor collides with the AMBs.

When the rotor collides with the AMBs, the power gas, which drive the expander wheel, are turned off, and the rotation speed of the rotor fall down. After

a short-time collision stage, the rotor operates normally again. However, it can be seen from Fig.6 that the curve in the process of rising speed do not accord with that in the process of falling speed. It is mainly caused by destroy of the balance precision of the rotor when it collides with the AMBs.

## CONCLUSION

Main results obtained in this paper are summarized as follows,

- (1) Both the values of the cylindrical and conical innate frequencies are sensitive to the control parameters, while the value of the first innate bending frequency is less sensitive.
- (2) The variation of the control parameters and the increase of the damping of the AMBs can restrain the vibration of the rotor when it rotates at the cylindrical and conical innate frequencies, while the damping of the AMBs is too little to keep the rotor rotating normally when the rotor operates near the beading innate frequency.

## ACKNOWLEDGEMENT

The financial support from the Jiangsu Province Natural Science Foundation of China under grant no. BK2003420 is gratefully acknowledged.

## REFERENCE

- [1] G. Schweitzer, H. Bleuler, A. Traxler, Active Magnetic Bearing, Zurich, vdf Hochschulverlag AG, 1994
- [2] Y.Hisanaga, O.Matsushita, S.Saitoh, Analysis and Evaluation of Unbalance Resonance Vibration and Bearing Reaction Force for Active Magnetic Bearing Equipped Flexible Rotor, Proc. of the 5<sup>th</sup> Int. Symp. on Magnetic Bearings, Kanazawa, Japan, August 1996, 71~76
- [3] Hirochika Ueyama, Helium Cold Compressor with Active Magnetic Bearings, Proc. of the 7<sup>th</sup> Int. Symp. on Magnetic Bearings, Zurich, Switzerland, August 2000, 1~6
- [4] Ming-chih Weng, Xiaodong Lu, David L. Trumper, Magnetic Suspension of Flexible Structures for Non-Contact, Proc. of the 7<sup>th</sup> Int. Symp. on Magnetic Bearings, Zurich, Switzerland, August 2000, 239~243
- [5] Juan Shi, Ron Zmood, Ijiang Qin, The Indirect Adaptive Feed-Forward Control in Magnetic Bearing Systems for Minimizing Selected Vibration Performance Measures, Proc. of the 8<sup>th</sup> Int. Symp. on Magnetic Bearings, Mito, Japen, August 2002, 223~228
- [6] Carl R. Knospe, R. Winston Hope, Stephen J. Fedigan, et al, New Results in the Control of Rotor Synchronous Vibration, Proc. of the 4<sup>th</sup> Int. Symp. on Magnetic Bearings, ETH, Zurich, August 1994, 119~124
- [7] Masujiro Hisatani, Tadao Koizumi, Adaptive Filtering for Unbalance Vibration Suppression, Proc. of the 4<sup>th</sup> Int. Symp. on Magnetic Bearings, ETH, Zurich, August 1994, 125~130
- [8] Felix Betschon, Carl Knospe, Gain Scheduled Adaptive Vibration Control, Proc. of the 7<sup>th</sup> Int. Symp. on Magnetic Bearings, Zurich, Switzerland, August 2000, 281~286
- [9] Yohji Okada, Disturbance Observer Based Controller for Flexible Rotor Supported by Magnetic Bearings, Proc. of the 4<sup>th</sup> Int. Symp. on Magnetic Bearings, ETH, Zurich, August 1994, 53~58
- [10] Yohji Okada, Takashi Saitoh, Yoshihiko Shinoda, Vibration Control of Flexible Rotor Supported by Inclination Control Magnetic Bearings, Proc. of the 6<sup>th</sup> Int. Symp. on Magnetic Bearings, Massachusetts, USA, August 1998, 702~709
- [11] M. Ohsawa, K. Yoshida, H. Ninomiya, et al, High-Temperature Blower for Molten Carbonate Fuel Cell Supported by Magnetic Bearings, Proc. of the 6<sup>th</sup> Int. Symp. on Magnetic Bearings, Massachusetts, USA, August 1998, 32~41